Inductive Grids in the Region of Diffraction Anomalies: Theory, Experiment, and Applications

PATRICK J. BLIEK, LINDSAY C. BOTTEN, ROGER DELEUIL, ROSS C. MC PHEDRAN, AND D. MAYSTRE

***Abstract*—We describe briefly a rigorous theory for the diffraction of a plane wave by inductive grids having circular apertures pierced in doubly periodic fashion in a thick, perfectly conducting screen. We compare the theory with measurements made at millimetric wavelengths, both for normal incidence and off-axis (in the region of strong polarization effects). We discuss the conclusions to be drawn from the calculations and measurements on the use of such grids as filters which pass short wavelengths, particularly in relation to their possible application in the field of solar energy.**

I. Introduction

INDUCTIVE and capacitive grids have long been of importance in the field of microwave engineering because of their applications as filters (high-pass, low-pass, and notch filters) [1], [2]. More recently, their application in the field of solar energy has been advocated, since there, one requires a device which can selectively absorb visible radiation and reject long wavelength [3]–[5]. In this second application it is particularly important to know the spectral behavior of the grid in the region of diffraction anomalies where the wavelength and grid period are of comparable order. Thus, it is of interest to have accurate theoretical models of grid behavior and to confirm these models with careful experimental measurements. As we will see, the behavior in the region of diffraction anomalies is critically dependent on the grid parameters, and so it is in this region that the most stringent tests of both the theoretical treatment and the experimental technique can be made.

Here, we describe briefly a rigorous theoretical model for the solution of the diffraction problem involving an inductive grid composed of circular apertures pierced in doubly periodic fashion in a thick, perfectly conducting screen (Fig. 1). The grid can be surrounded by a symmetric dielectric sandwich and the apertures can be plugged with a second dielectric. (It would pose no extra theoretical difficulties to treat the case of lossy plug and sandwich materials, but we are interested in studying a transparent heat mirror in which absorption of radiation into the grid is undesirable.)

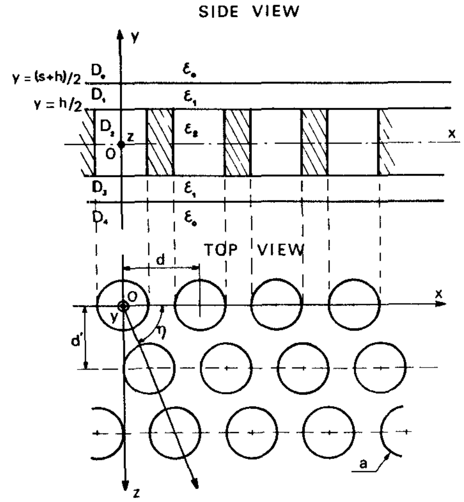

Fig. 1. The geometry of the round-holed inductive grid.

We will also describe an experimental investigation into the behavior of the bare grid, conducted in the microwave region (the frequency lying between 26.5 GHz and 40 GHz). Both measurements at constant wavelength and constant angle of incidence are presented. Preliminary comparisons between theory and experiment have been presented elsewhere [6].

II. Theoretical Model

The theoretical formalism which we have used to solve the diffraction problem of Fig. 1 is based upon the work of Chen [2], [7], [8]. Note that the structure of Fig. 1, while being more general than the geometries studied by Chen, is capable of still further generalization without increasing the complexity of the formalism. For example, any number of plane dielectric or absorbing films could be placed above and below the grid. The structure need not have the up–down symmetry shown in Fig. 1, but this assumption

Manuscript received March 27, 1980; revised June 12, 1980. This work was supported in part by the Science Foundation for Physics of the University of Sydney, Sydney, Australia, and in part by the Australian Research Grants Committee.

P. J. Bliek and R. Deleuil are with the Laboratoire de Radioélectricité, Faculté de St-Jérôme, Université de Provence, 13397, Marseille, France.

L. C. Botten is with the School of Mathematical Sciences, The New South Wales Institute of Technology, P.O. Box 123, Broadway, N.S.W., 2007, Australia.

R. C. Mc Phedran is with the Department of Theoretical Physics, University of Sydney, Sydney, N.S.W., 2006, Australia.

D. Maystre is with Laboratoire d'Optique Electromagnétique, E.R.A. au CNRS No. 597, Faculté de St-Jérôme, Université d'Aix-Marseille III, 13397, Marseille, France.

0018-9480/80/1000-1119$00.75 ©1980 IEEE

enables a significant reduction in computing time. Only an outline of the theory will be presented here. More detailed descriptions are available elsewhere [9], [10].

We consider a plane wave of wavelength λ incident upon a doubly periodic structure consisting of circular apertures pierced in a plane, perfectly conducting screen (Fig. 1). The various media D_i associated with the grid structure are taken to be dielectrics of refractive index r_i (where $r_i^2=\epsilon_i/\epsilon_0$). The grid has two axes of periodicity making an angle η with one another.

The direction of the incident wave in the free space region (D_0) is specified by the spherical polar angles ϕ, ψ. Here ϕ is the angle of declination measured from the positive y axis, while ψ is the azimuthal angle measured in a clockwise sense from the x axis of Fig. 1. The polarization of the wave is specified by a third angle δ, such that a TE wave corresponds to $\delta=0°$ while a TM wave corresponds to $\delta=90°$. (Here transverse means the absence of an $0y$ component of the relevant field).

In regions D_0, D_1, D_3, and D_4 we expand the necessary field components (i.e., those in the xz plane) in series of plane waves. The directions of propagation of the plane waves are given by grating equations, generalized to two dimensional structures (see, for example, Chen [2]). The xz components of the fields in region D_2 are expressed as sums of cylindrical waveguide modes (see, for example, Marcuvitz [11]). Both the "horizontal" and "vertical" orientations of the TE and TM modes must, in general, be included in the field expansions.

The diffraction problem is solved by matching the tangential components of the electric and magnetic fields between D_2 and D_1, D_3. The method of moments is then used to reduce the resulting functional equations to systems of linear equations, which are solved using standard elimination techniques. Analytic expressions for the inner products of plane wave terms with waveguide modes may be found in Amitay and Galindo [12].

In the computer implementation of the method, up to 225 plane waves and up to 50 waveguide modes can be included. The criterion of conservation of energy is analytically satisfied by the program results, as a result of the structure of the linear equations in the formalism [13]. The Reciprocity Theorem does provide a valuable check on the magnitude of errors resulting from truncation of field expansions. The relevant form of this constraint for grids is given in [5], [14]. Also an amplitude constraint [15], [16] for a particular configuration of incident and diffracted beams may be used as a check on the accuracy of results. The numerical results presented below are accurate to better than 2 percent as assessed by the above criteria and also by their convergence with increasing numbers of plane waves and modes.

III. Comparison of Theory and Experiment

Measurements were made in the millimetric region (more precisely in the K_a band, i.e., 0.75 cm $\leqslant \lambda \leqslant$ 1.13 cm). The choice of this range of wavelengths was made basically for two reasons. Firstly, it is possible to make with high precision crossed gratings of acceptable size in a metallic material which, in this wavelength band, can legitimately be considered as perfectly conducting. Secondly in this frequency range there exists at Marseille at the Laboratoire de Radioélectricité an experimental apparatus for measuring diffraction or diffusion effects. This apparatus has already been used for numerous studies, both in the radio-wave region [17] and also in that of optical-analog measurements [18], [19], and has shown itself very powerful.

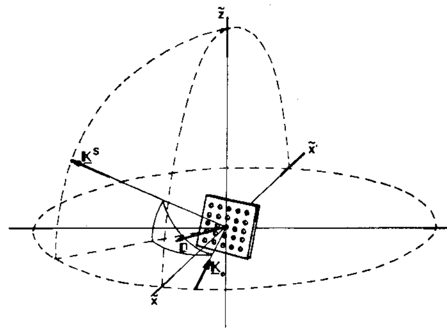

Fig. 2. Schematic representation of the device: $0\tilde{x}\tilde{y}\tilde{z}$ axis are linked with anechoic chamber and must not be confused with $0xyz$ axis. $\boldsymbol{K}^s$ denotes the wave vector of a scattered wave. The incident wave vector $\boldsymbol{K}_0$ is fixed. On the other hand the normal $\boldsymbol{n}$ at the grating can be arbitrarily oriented and the detector (reception antenna) can be located at any point of the radioelectrical sphere.

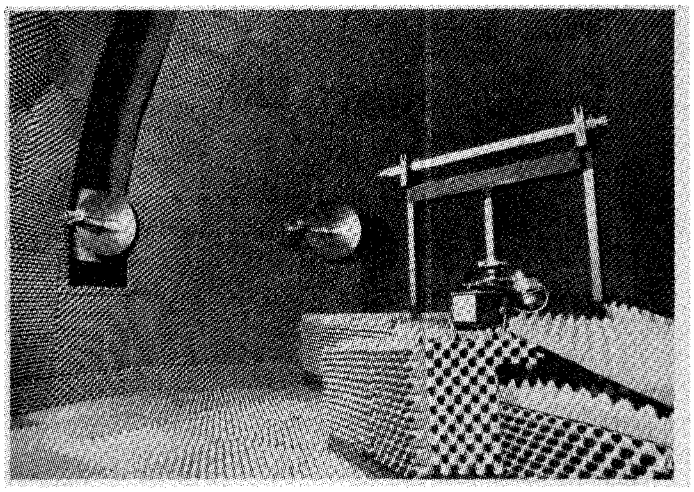

Fig. 3. Anechoic chamber for target tests in K_a band.

In essence, the equipment consists of a goniometer of radius 3 m, placed in an anechoic chamber with an isolation better than 40 dB (Fig. 2 and 3) [17]. The antennae for emission and reception were parabolic mirrors of diameter $D=0.53$ m ($D\simeq 60\ \lambda$); this gave a high gain and permitted the use of large grids (0.30 m$\times$0.26 m). Thus it is possible to use grids, having thousands of apertures, which can be realistically considered as being infinite in extent [20]. The orientation of the primary source (horn) of the paraboloid of emission controls the polarization of the incident wave. It is then possible to work successively in the two principal cases of polarization, called $E_{//}$ ($\delta=90°$) or $E_{\perp}$ ($\delta=0°$), according as to whether the incident electric field is parallel or perpendicular to the plane of incidence.

The phenomena to be studied here (filtering and resonance effects) extend over a wavelength range which exceeds the usable K_a band. Thus we have been forced to construct three isomorphic grids whose characteristics are given in Table I. It is then possible to vary the ratio of the wavelength to the grating period (λ/d) between 0.8 and 2.2. The measurements were made using a 1753 phase-amplitude receiver, a 1833-20 ratiometer, and a 1523 chart recorder of "Scientific-Atlanta".

The system of data acquisition and analysis is performed by a "Hewlett-Packard 9825" minicomputer. Each measurement consists of the determination firstly of the diffracted power P_{pq} (or $\hat{P}_{pq}$) diffracted by reflection (or by transmission) by the grid into the given order (p,q) and secondly of the incident power P_i. The efficiency of the transmitted order (p,q) is then given by

$$\hat{\rho}_{p,q}=\frac{\hat{P}_{p,q}}{P_i}.$$

The relative error of a power measurement is smaller than 1.5 percent and so the relative accuracy of the efficiency is better than 3 percent. Both normal incidence and off axis measurements of transmitted energy were performed, the latter being made in order to investigate the strong polarization effects consequent upon breaking the square symmetry existing for normal incidence.

A. Measurements at Normal Incidence

In Fig. 4 we compare a theoretical curve for the energy transmission by the isomorphic grids of Table I with the experimental measurement. The agreement is excellent at all save one of the points. Repeated attempts both theoretically and experimentally have not succeeded in reducing the discrepancy at this point. However, it should be noted that it is the first of the five-points obtained with grid 1. This is the thinnest of the three grids, and the only one with noticeable departures from planarity caused by its manufacture. We attribute the discrepancy to the effect of the nonplanarity on the shape of the wavefront of the transmitted zeroth order.

It will be noted that the experimental points confirm well the theoretical predictions concerning the Wood and resonance anomalies [21]. The first of these occur at any wavelength at which a diffracted order ceases to propagate. For normally incident light, Wood anomalies for a grid having $\eta=90°$ and $d=d'$ occur at normalized wavelengths

$$\lambda_R(p,q)/d=1/\sqrt{p^2+q^2}\,. \qquad (1)$$

At $\lambda/d=1.0$ the four orders $(\pm 1,0)$ and $(0,\pm 1)$ cease to propagate. Below this wavelength they can carry reflected energy away from the top surface of the grid. It is the energy carried by these waves which is responsible for the abrupt drop in the transmitted energy curve at $\lambda/d=1.0$.

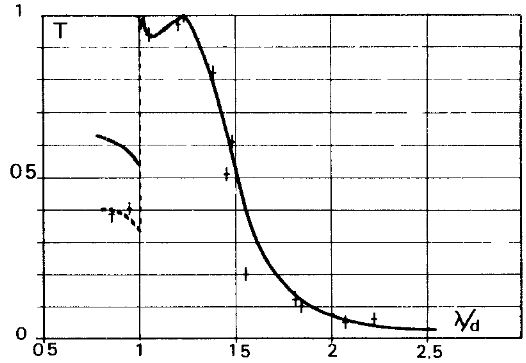

Fig. 4. A theoretical curve for the energy transmitted (T) by the isomorphic grids of Table I as a function of normalized wavelength. The dashed curve for $\lambda/d<1.0$ gives the zeroth order efficiency $\hat{\rho}_{00}$. The crosses are the experimental measurements.

TABLE I

CHARACTERISTICS OF THE THREE ISOMORPHIC GRIDS USED IN THE MEASUREMENTS

Number of the grid	1	2	3
Groove spacing d (mm)	5	7.5	10
Diameter of the holes a (mm)	4.5	6.75	9
Thickness of the metal h (mm)	2	3	4
Number of holes	3120	1360	780

The resonance anomaly peaks at $\lambda/d=1.25$ and corresponds to the resonant frequency of the equivalent circuit of the grid [1]. The filtering region of the grid occurs on the long-wavelength side of this anomaly.

B. Off-Axis Measurements

Fig. 5 shows the variation of the transmitted (0,0) order efficiency with angle of incidence ϕ at a fixed normalized wavelength of $\lambda/d=1.12$ for grid 2. Although the energy properties of the grid are polarization independent at normal incidence ($\phi=0$), the effects of polarization become apparent in a remarkably rapid manner as one moves off axis. It is astonishing that a variation of only 6° can transform a structure from being polarization independent to one being a good polarizer. This strong polarization effect is caused by the presence of the $(0,-1)$ Wood anomaly ($\phi_R=6.5°$).

In the case of $E_{\perp}$ polarization, the agreement between theory and experiment is almost perfect. The Wood anomaly is evident only as a change in the gradient of the curve. However for $E_{//}$ polarization, the experiment shows the anomaly as being an abrupt loss of energy from the transmitted spectrum, this energy plunging by 80 percent in 2°! In the narrow angular band ($6.2°\leqslant\phi\leqslant 6.8°$) numerical convergence is particularly difficult to achieve

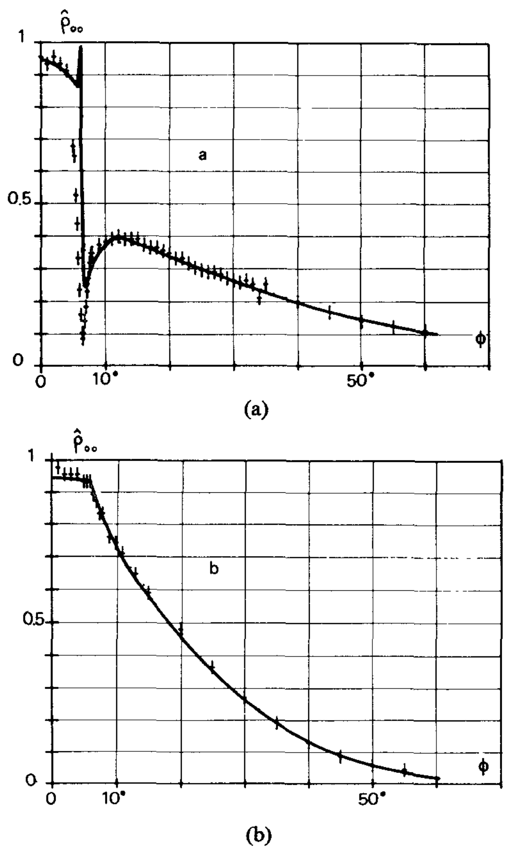

Fig. 5. Transmitted energy $\hat{\rho}_{00}$ in the order (0,0) as a function of angle of incidence (ϕ) for grid 2. Here $\lambda/d=1.12$ and $\psi=90°$. (a) $E_{//}$ case. (b) $E_{\perp}$ case. The crosses are the experimental measurements.

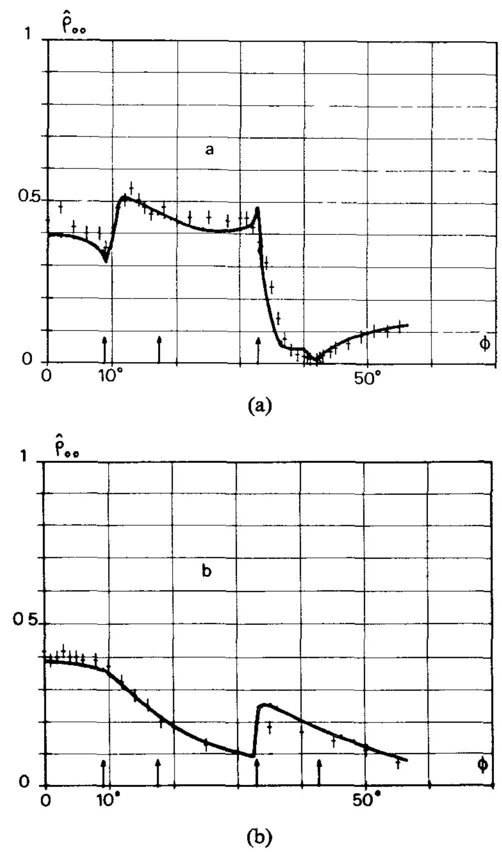

Fig. 6. The same as Fig. 5 except $\lambda/d=0.84$; the passing off of diffracted orders are pointed out by arrows.

because of the very rapid fluctuation in the distribution of the transmitted energy carried by the various modes in the grid apertures.

In Fig. 6 we present corresponding curves for a shorter normalized wavelength of $\lambda/d=0.84$. Four Wood anomalies occur in the angular range of $0°<\phi<60°$, corresponding to the passing off of orders (0,1) at 9.2°, $(\pm 1,-1)$ at 17.3°, $(\pm 1,0)$ at 32.9°, and $(0,-2)$ at 42.8°. Of these the $(\pm 1,0)$ anomaly is the most pronounced for both fundamental polarizations. Once again, agreement between theory and experiment is seen to be excellent.

IV. Solar Selectivity of Round-Holed Grids

In this section we present the results of our study involving the use of such grids as solar selective elements placed in front of a black body absorber. In reference [5] a thorough analysis of the spectral properties of grids having rectangular apertures was presented. Here, we will not attempt such a comprehensive examination but will confirm the applicability (to grids with circular apertures) of the properties found in [5]. Furthermore, we examine in some detail the improvement gained by sandwiching the structure within a dielectric film pair and by inserting a dielectric plug.

A. Grids Without Plugs and Films

It has been shown [5] that the solar transmittance of grids is closely related to the hole-area fraction (HAF). For the case of circular apertures whose diameter is 90 percent of the fundamental grid period the hole-area fraction corresponding to orthogonal periodicity axes is 63.6 percent. If the apertures are arranged to lie on the vertices of an equilateral triangle ($\eta=60°$) the HAF can be raised to 73.5 percent. In Fig. 7(a) and 7(b) we show transmission curves for grids having aperture arrangements as described above and in Table II we present the optimum solar absorptance values for the grids. (Here the optimum has been achieved by varying the grid period and hence rescaling the efficiency spectrum in order to obtain maximum integrated solar absorptance). The superiority of the grid having a more closely packed arrangement of apertures is evident. Note that the equilateral triangle arrangement has two axes of the periodicity parallelogram at right angles to one another and so its transmission is independent of the polarization angle (δ) for normally incident radiation.

We have computed the transmission curve for a grid having the same HAF as the grid of Fig. 7(a), but with $\eta=60°$ rather than 90°. The solar transmission values for the two grids are very similar, confirming that it is the HAF rather than the placement of apertures which is important.

We have examined the spectral characteristics of a grid identical to that of Fig. 7(b) but with its thickness slightly smaller ($h/d=0.3$). The curves are similar, as are the solar transmission values. This grid exhibits weaker anomalies

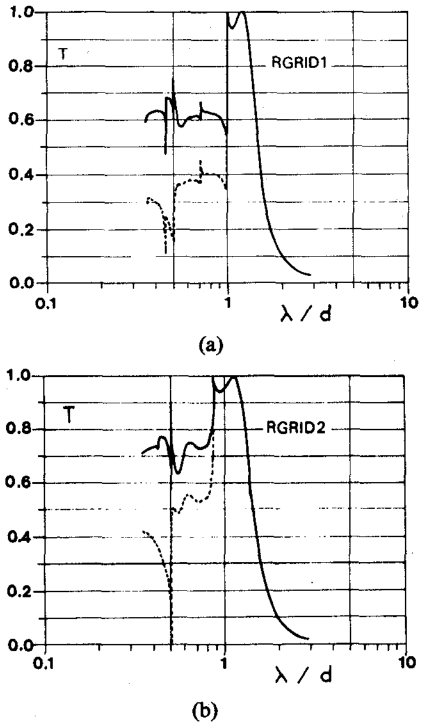

Fig. 7. Transmittance as a function of normalized wavelength for the two grids of Table II. (Normal incidence $\phi=0°, \psi=\delta=90°$). The solid curve denotes the total transmittance, while the dashed curve refers to that of the order (0,0). (a) RGRID 1. (b) RGRID 2.

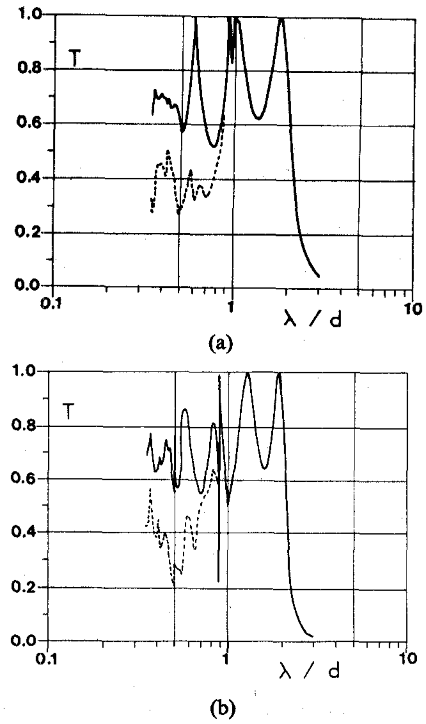

Fig. 8. (a) Transmittance as a function of normalized wavelength for RGRID2, with a dielectric plug of refractive index 1.5. (b) Transmittance for a similar structure, but with a normalized thickness of 0.6.

TABLE II
INTEGRATED SOLAR TRANSMITTANCE FOR BARE GRIDS

Grid Description	Optimal Period (d, μm)	Integrated (%) Transmittance
RGRID 1 (a/d = 0.45, h/d = 0.4, η = 90°) (Fig. 8(a))	1.0	64.1
RGRID 2 (a/d = 0.45, h/d = 0.4, η = 60°) (Fig. 8(b))	1.2	74.5

and a diminished long wavelength filtering action because of its smaller thickness, as was found for grids with square apertures [5].

Finally we have studied the behavior of the optimal grid (RGRID2) when operated off axis. As in [5] we have found that the strong polarization dependence in such configuration markedly reduces the integrated solar transmittances. Thus it is imperative to use these grids in direct illumination and to have their surface normal directed towards the sun.

B. Grids with Plugs Only

Let us consider the effect on the performance of the optimal grid of introducing plugs of refractive index 1.5 in place of air in the circular apertures. As can be seen by comparison of Figs. 7(b) and 8(a) the presence of the plug has the effect of broadening and complicating the resonance region of the transmission curve. The single resonance peak of Fig. 7(b) for $\lambda/d > 1.0$ is split into a pair of resonance peaks. As Fig. 8(b) shows, these move away from the Wood anomaly at $\lambda/d = 0.866025$ towards longer wavelengths with increasing optical thickness of the plug. Further increases in the optical depth would be expected to result in the creation of additional grid resonances.

Another aspect of the performance illustrated by Fig. 8(a) and 8(b) is the frequency and strength of the diffraction anomalies occurring in the transmission region, $\lambda/d < 0.866025$. This we attribute to the greater number of waveguide modes capable of propagating (ν_{nm} real) for a given wavelength. The frequency of the anomalies makes difficult the characterization of convergence over the entire spectrum using only a restricted set of sample points. However this is not of great importance as the anomalies would tend to be greatly smoothed in any experimental situation because of inevitable imperfections of manufacture and measurement. The solar absorptance of the grids

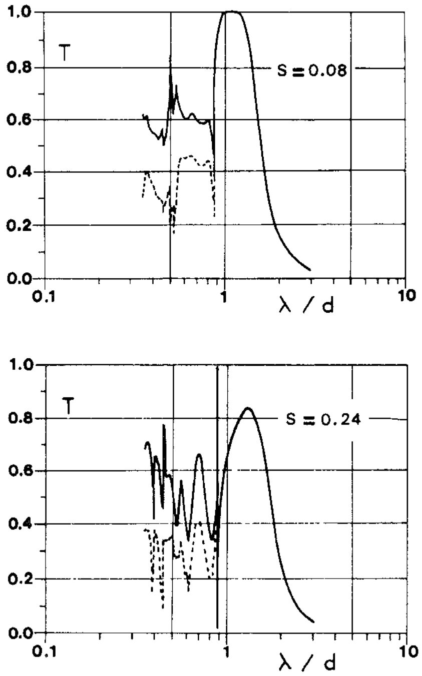

(b)

Fig. 9. Transmittance as a function of wavelength for RGRID2 surrounded by symmetric dielectric sandwiches of varying thickness, each of refractive index 1.5. (a) $s/d=0.08$. (b) $s/d=0.24$.

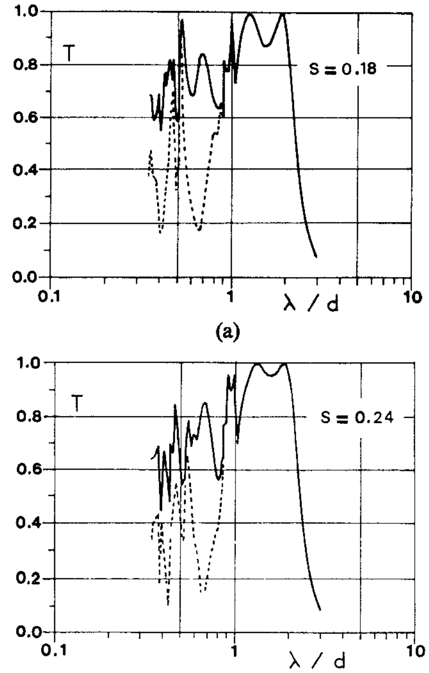

(b)

Fig. 10. Transmittance as a function of wavelength for RGRID2 plugged with a dielectric of refractive index of 1.5 and surrounded by symmetric films of varying thickness each having a refractive index of 1.5. (a) $h/d=0.18$. (b) $h/d=0.24$.

TABLE III
INTEGRATED SOLAR TRANSMITTANCE FOR RGRID2, WITH A PLUG OF REFRACTIVE INDEX 1.5, AS A FUNCTION OF TOTAL SANDWICH THICKNESS (THE SANDWICH REFRACTIVE INDEX BEING ALSO 1.5)

Normalized Sandwich Thickness (s/d)	Optimal Period (d,μm)	Integrated Transmittance (%)
0.0	1.0	70.7
0.18	0.5	81.0
0.24	0.5	83.5

shown in Fig. 8(a) and 8(b) is several percent lower than that of Fig. 7(b). Nevertheless, we have noted that the insertion of plugs has had the potentially beneficial effect of widening the resonance region.

C. Grids with Films Only

In this section we examine the behavior of the optimal grid with a symmetric sandwich of dielectric material (refractive index of 1.5) surrounding it. The performance for sandwich thicknesses of 0.08 and 0.24 by the grid period is shown in Fig. 9(a) and 9(b). We note that nonzero sandwich thickness leads to lower performance in the transmission region, and also to frequent and strong anomalies there. These anomalies have three sources.

1) Wood anomalies—arising when propagating orders in the sandwich become evanescent. Because of the refractive index of the film, it is possible to support a higher number of propagating orders than in air with the consequence of more frequent anomalies.

2) Grid resonance anomalies—arising within the aperture regions, which are now leaky resonant cavities. The presence of the sandwich layer bounding the air filled cavity represents an additional impedance mismatch with consequent reflection losses. It is these losses which are responsible for the lowering of the mean transmission value in this region.

3) Thin film interference fringes—become more evident as the optical thickness of the sandwich increases.

The encouraging feature evident in Fig. 9 is that the introduction of the sandwich structure has enabled us to eliminate the resonance dip occurring just after the final Wood anomaly. It was this dip which lowered the transmission in the resonance region for grids with plugs only. Consequently, we deduced that a combination of the plug and sandwich structures would lead to a performance possessing and enhanced bandwidth.

D. Grids with Both Films and Plugs

We present in Fig. 10 two curves illustrating the changes in grid behavior with varying sandwich thickness for a fixed plug thickness. The refractive index of the plug has been chosen to be equal to that of the sandwich in order to minimize reflection losses at their interface. The performance figures shown in Table III for these grids illustrate the great improvement in solar transmittance which has been achieved by the modification of the grid geometry suggested above. It will be noted that the optimal performance is achieved for grid periods around 0.5 μm, whereas for the unmodified grid it was approximately 1.0 μm. This change has come about because the resonance region has been incorporated into the transmission region. For the first time we have been able to surpass the geometrical optics limit (the hole-area fraction) on the transmittance.

V. Conclusions

The study of the round-holed grid represents a good example of a simultaneous and coordinated attack by theoreticians and experimenters on a problem of practical importance. The agreement between theory and experiment is of such a quality as to permit various applications of the formalism to be made with confidence.

We have already studied the performance of these grids as solar selective elements (i.e., in the wavelength domain, as low pass filters). We show here that, despite the relatively low hole-area fractions possible with circular apertures, the use of dielectric plugs and sandwiches as impedance-matching elements permits us to obtain good solar selectivity.

It should be noted that the improvements in performance obtained with plugs and films for this grid were significant only because of the low hole-area fractions. We have tried [10] to improve the performance of the optimal square-holed solar selective grid of reference [5] using this technique, but the resulting improvements so derived were only of a marginal nature. We believe that the technique is only appropriate to those geometries whose transmission bandwidth is low.

This confrontation between theory and experiment represents the first such comparison for grids in the zone of their diffraction anomalies. Given the vastly increased difficulty of the theoretical processes for such grids when compared with those for usual diffraction gratings, the quality of the agreement described here is very encouraging.

Acknowledgment

This work was in part performed while one of the authors (R. C. McP.) was the guest of Prof. R. Petit at the Laboratoire d'Optique Electromagnétique at Marseille. He thanks him for his hospitality and acknowledges also the Australian Research Grants Committee and the Science Foundation for Physics in the University of Sydney for provision of funds and facilities.

References

[1] R. Ulrich, "Far-infrared properties of metallic mesh and its complementary structure," *Infrared Phys.*, vol. 7, pp. 37–55, Jan. 1967.

[2] C. C. Chen, "Transmission through a conducting screen perforated periodically with apertures," *IEEE Trans. Microwave Theory Tech.*, vol. 18, pp. 627–632, Sept. 1970.

[3] C. M. Horvitz, "A new solar selective surface," *Opt. Commun.*, vol. 11, pp. 210–212, June 1974.

[4] J. C. C. Fan, F. J. Bachner, and R. A. Murphy, "Thin-film conducting microgrids as transparent heat mirrors," *Appl. Phys. Lett.*, vol. 28, pp. 440–442, Apr. 1976.

[5] R. C. Mc Phedran and D. Maystre, "On the theory and solar application of inductive grids," *Appl. Phys.*, vol. 14, pp. 1–20, Sept. 1977.

[6] R. C. Mc Phedran, L. C. Botten, P. Bliek, R. Deleuil, and D. Maystre, "Theoretical and experimental studies of inductive grids," presented at the 8th European Microwave Conf. (Paris, France), Sept. 4–8, 1978.

[7] C. C. Chen, "Diffraction of electromagnetic waves by a conducting screen perforated periodically with circular holes," *IEEE Trans. Microwave Theory Tech.*, vol. 19, pp. 475–481, May 1971.

[8] C. C. Chen, "Transmission of microwaves through perforated flat plates of finite thickness," *IEEE Trans. Microwave Theory Tech.*, vol. 21, pp. 1–6, Jan. 1973.

[9] R. C. Mc Phedran and L. C. Botten, "Inductive grids with circular aperture," Internal Rep. SP77/5, School of Physics, The University of Sydney, Sydney, Australia, Aug. 1977.

[10] L. C. Botten, "Theories of singly and doubly periodic diffraction gratings," Ph.D. thesis, The University of Tasmania, Feb. 1978.

[11] N. Marcuvitz, *Waveguide Handbook*. New York: McGraw-Hill, 1951, ch. 2, pp. 66–72.

[12] N. Amitay and V. Galindo, "On the scalar product of certain circular and Cartesian wave functions," *IEEE Trans. Microwave Theory Tech.*, vol. 16, pp. 265–266, Apr. 1968.

[13] N. Amitay and V. Galindo, "On energy conservation and the method of moments in scattering problems," *IEEE Trans. Antennas Propagat.*, vol. 17, pp. 747–751, Nov. 1969.

[14] G. H. Derrick, R. C. Mc Phedran, D. Maystre, and M. Nevière, "Crossed gratings: A theory and its applications," *Appl. Phys.*, vol. 18, pp. 39–52, Jan. 1979.

[15] L. C. Botten, "A new formalism for transmission gratings," Opt. Acta, vol. 25, pp. 481–499, June 1978.

[16] J. L. Adams, L. C. Botten, and R. C. Mc Phedran, "The crossed lamellar transmission grating," J. Opt. (Paris, France), vol. 9, pp. 91–100, Mar. 1978.

[17] P. Bliek, R. Deleuil, and J. P. Marcellin, "Recherches expérimentales dans le domaine des microondes sur des cibles radioélectriques ou sur des modèles de surfaces optiques destinées à des applications solaires," *Ann. Télécom.*, submitted for publication.

[18] R. Deleuil, "Réalisation et utilisation d'un appareillage destiné à l'étude des dioptres irréguliers et des réseaux en ondes millimétriques," *Opt. Acta*, vol. 16, pp. 23–35, Jan. 1969.

[19] A. Wirgin and R. Deleuil, "Theoretical and experimental investigations of a new type of blazed grating," *J. Opt. Soc. Amer.*, vol. 59, pp. 1348–1357, Oct. 1969.

[20] C. H. Palmer, F. C. Evering, and F. M. Nelson, *Appl. Opt.*, vol. 4, pp. 1271–1281, 1965.

[21] E. G. Loewen, D. Maystre, R. C. Mc Phedran, and I. J. Wilson, "Correlation between efficiency of diffraction gratings and theoretical calculations over a wide range," *Japan J. Appl. Phys.*, vol. 14, suppl. 14-1, pp. 143–152, 1974.